

E. A. Ogryzlo and
Gerald B. Porter

University of British Columbia
Vancouver, Canada

Contour Surfaces for Atomic and Molecular Orbitals

Models of atoms which show electrons moving in well defined orbits around the nucleus are not consistent with a vast body of experimental evidence or with current theories of atomic structure. The wave mechanical description of the electron in an atom arose from de Broglie's (1) wave theory of matter, and is contained in a wave equation proposed by Schrödinger (2) in 1926 (the symbols are defined in (5)):

$$\nabla^2\psi + \frac{8\pi^2\mu}{h^2}(E - V)\psi = 0$$

The equation describes a standing wave, and if some physical picture of the electron is to be retained an interpretation of ψ (wave function) in terms of some property of the electron is essential.

Since in Maxwell's wave theory of light ψ^2 was successfully related to the intensity of a light beam, Schrödinger (2) initially suggested that ψ^2 for an electron was a measure of its density at any point. A few months later, Max Born (3) gave the presently accepted interpretation of ψ . In view of the Heisenberg uncertainty principle (4), Born identified ψ^2 (or $\psi^*\psi$, i.e., the wave function times its complex conjugate when ψ contains imaginary parts) with the probability of finding the electron at that point. It is interesting to notice that the concept of a moving electron nowhere enters the description given by the Schrödinger equation, and in fact it is not possible to conceive of any classical motion that would result in most of the probability distributions that arise. Nevertheless, because the probability function ($\psi^*\psi$) is not time dependent, models of the atom in various stationary states can be constructed.

The ideal model of an atomic or molecular orbital would be a cloud-like structure showing the probability of finding an electron at all points in space relative to the nucleus. Although it is conceivable that a model could be made with a colored suspension in a clear plastic, the difficulty of preparing such a model precludes its use. Somewhat less effective, but more easily constructed models can be fashioned from styrofoam to represent contour surfaces. The surface visible must then represent a contour surface of constant ψ (wave function) or of constant $\psi^*\psi$ (probability function). There are a number of ways in which the surface could be labeled, e.g., (a) by the value of ψ relative to ψ_{\max} , (b) by the value of $\psi^*\psi$ compared with $\psi^*\psi_{\max}$, (c) by the fraction of $\psi^*\psi$ enclosed by the contour surface.

The last method is probably the most effective for labeling the surface since it gives the probability of finding the electron within the surface, or, as a less correct alternative, the fraction of the electron(s) enclosed by the contour surface. For purposes of computation it is more convenient to use method (b). We

will now present a method by which contour surfaces can be calculated, and show how these can be used to construct some models that are useful for introductory courses in atomic and molecular structure.

Atomic Orbital Contour Surfaces

Cohen (4) has shown that these contours for a p orbital can be found by expressing the wave function in Cartesian coordinates and separating the variables. This cannot be done in general; hence it is appropriate to use polar coordinates in which the variables are always separable. The function $\psi^*\psi$ is given in Table 1 for a number of atomic orbitals. Strictly, these are correct only for "one electron" atoms, but are extended to the general case of a many electron atom by using an effective nuclear charge, Z , for a particular orbital (6). Though the effective nuclear charge varies with r we shall use an average value to make the calculations less formidable.

The method of obtaining contours will be developed in detail for the $3d$ orbitals of Ti(III), which has $Z \approx 9.2$. We consider first a $3d_{x^2-y^2}$ orbital, the contours of which are identical with those of the $3d_{xy}$, $3d_{xz}$ and $3d_{yz}$ orbitals except for their direction in the coordinate system. The electron density, $\psi^*\psi$, along the x axis, shown in Figure 1, is calculated from the appropriate function of Table 1 with $\theta = 90^\circ$ and $\phi = 0^\circ$. The contours of constant electron density are different in the xy and xz planes, and must be evaluated separately.

In the xy plane, we have, with $\theta = 90^\circ$:

$$(\psi^*\psi)_{xy} = \frac{1}{3^8 2\pi} \left(\frac{Z}{a}\right)^3 \sigma^4 e^{-(2\sigma/3)} \cos^2 2\phi$$

in which a is the Bohr radius (0.529 \AA), and $\sigma = Zr/a$. It is convenient to assume values of σ and calculate values of ϕ which give a chosen value of $\psi^*\psi$. This has been done for $\psi^*\psi$ equal to 0.316 and 0.10 of the maximum $\psi^*\psi$, with the results given in Figure 2. The same result can be found by a graphical solution

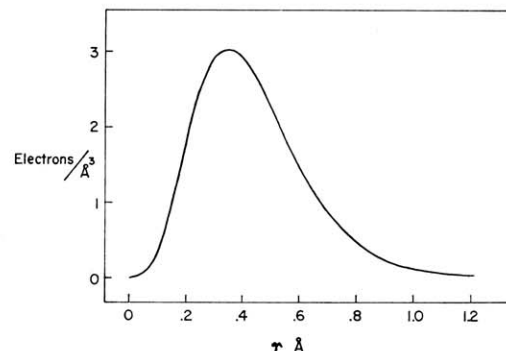


Figure 1. Electron density in a Ti(III) $3d_{x^2-y^2}$ orbital along the x (or y) axis.

employing the curve of Figure 1. The nodes ($\psi^*\psi = 0$) are found at values of ϕ that make $\cos^2 2\phi$ equal to zero ($\phi = 45^\circ$, etc.).

The same procedure in the xz plane ($\phi = 0$) develops solutions of

$$(\psi^*\psi)_{xz} = \frac{1}{3^{8/2}\pi} \left(\frac{Z}{a}\right)^3 \sigma^4 e^{-2\sigma/3} \sin^4 \theta$$

with the results shown in Figure 3. Thus the contour surfaces of the $d_{x^2-y^2}$ orbital are oval in cross section (see models in Fig. 11).

The $3dz^2$ orbital is independent of ϕ (see Table 1) hence the contour surfaces have cylindrical symmetry about the z axis. The electron density distribution

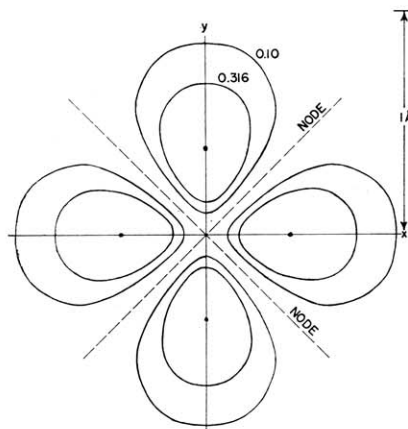


Figure 2. Contours of constant ψ^2 at 0.10 and 0.316 of maximum for a Ti(III) $3d_{x^2-y^2}$ orbital in the xy plane. There are two nodal planes perpendicular to the paper and bisecting the axis.

along the z axis is identical with that of Figure 1, except that the magnitude of the density is larger by a factor $4/3$. The contours are given in Figure 4 for the same fractions of the maximum electron density as above, although for the "doughnut" in the xy plane, the electron density does not reach 0.316 of the maximum. Nodes are found at $\theta = \cos^{-1}(1/3)^{1/2} = \pm 55^\circ$.

A similar treatment for the $3p_z$ orbital of the chlorine atom ($Z \approx 6.1$) gives the electron density (along the z axis) shown in Figure 5 and the contour lines in Figure 6. The contour surfaces can be generated by rotation of this curve around the z axis. Aside from a node in the xy plane there is also a spherical node of radius $\sigma = 6$ or $r = 0.52$ Å. Similar curves are shown in Figures 7 and 8 for the $2p_z$ orbital of a carbon atom, previously treated by Cohen (4).

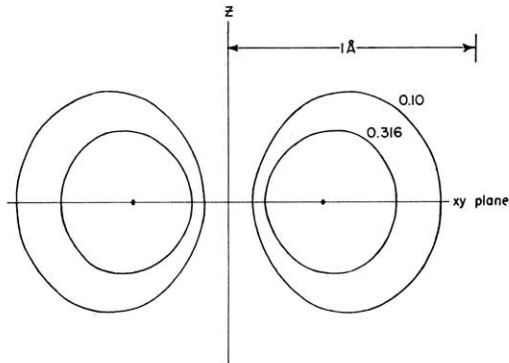


Figure 3. Contours of constant ψ^2 at 0.10 and 0.316 of maximum for a Ti(III) $3d_{x^2-y^2}$ orbital in the xz plane. The z -axis is the intersection of the two nodal planes shown in Figure 2.

Table 1. Probability Functions for Hydrogen-Like Atoms

| n | l | m | Orbital | $\psi^*\psi$ |
|-----|-----|-----|-----------|--|
| 1 | 0 | 0 | 1s | $\frac{1}{\pi} (z/a)^3 e^{-\sigma}$ |
| 2 | 0 | 0 | 2s | $1/(2^5 \pi) (z/a)^3 (2 - \sigma^2) e^{-\sigma}$ |
| | 1 | 0 | $2p_0$ | $1/(2^5 \pi) (z/a)^3 \sigma^2 e^{-\sigma} \begin{cases} \cos^2 \theta \\ \sin^2 \theta \\ \sin^2 \theta \end{cases}$ |
| | | +1 | $2p_{+1}$ | |
| | | -1 | $2p_{-1}$ | |
| | 0 | 0 | 3s | $1/(3^8 \pi) (z/a)^3 (27 - 18\sigma + 2\sigma^2)^2 e^{-(2\sigma/3)}$ |
| | 1 | 0 | $3p_0$ | $2/(3^8 \pi) (3/a)^3 (6 - \sigma)^2 \sigma^2 e^{-(2\sigma/3)} \begin{cases} \cos^2 \theta \\ \sin^2 \theta \\ \sin^2 \theta \end{cases}$ |
| 3 | 0 | +1 | $3p_{+1}$ | |
| | | -1 | $3p_{-1}$ | |
| | 2 | 0 | $3d_0$ | $\frac{1}{(2)^{10} \pi} (z/a)^3 \sigma^4 e^{-(2\sigma/3)} \begin{cases} 1/3 (3 \cos^2 \theta - 1)^2 \\ 4 \sin^2 \theta \cos^2 \theta \\ 4 \sin^2 \theta \cos^2 \theta \\ \sin^4 \theta \\ \sin^4 \theta \end{cases}$ |
| | | +1 | $3d_{+1}$ | |
| | | -1 | $3d_{-1}$ | |
| | | +2 | $3d_{+2}$ | |
| | | -2 | $3d_{-2}$ | |

An Alternative Orthogonal Set of p Orbitals

$$\begin{aligned} &\psi 2p_{+1} + i\psi 2p_{-1} & 2p_x & \frac{1}{2^5 \pi} (z/a)^3 \sigma^2 e^{-\sigma} \begin{cases} \sin^2 \theta \cos^2 \phi \\ \sin^2 \theta \sin^2 \phi \\ \cos^2 \theta \end{cases} \\ &\psi 2p_{+1} - i\psi 2p_{-1} & 2p_y & \\ &\psi 2p_0 & 2p_z & \end{aligned}$$

An Alternative Orthogonal Set of d Orbitals

$$\begin{aligned} &\psi 3d_0 & 3d_x^2 & \frac{1}{(2)^{10} \pi} (z/a)^3 \sigma^4 e^{-(2\sigma/3)} \begin{cases} 1/3 (3 \cos^2 \theta - 1)^2 \\ 4 \sin^2 \theta \cos^2 \theta \cos^2 \phi \\ 4 \sin^2 \theta \cos^2 \theta \cos^2 \phi \\ \sin^4 \theta \sin^2 2\phi \\ \sin^4 \theta \cos^2 2\phi \end{cases} \\ &\psi 3d_{+1} + i\psi 3d_{-1} & 3d_{xz} \\ &\psi 3d_1 - i\psi 3d_{-1} & 3d_{yz} \\ &\psi 3d_{+2} + i\psi 3d_{-2} & 3d_{xy} \\ &\psi 3d_{+2} - i\psi 3d_{-2} & 3d_{(x^2-y^2)} \end{aligned}$$

where

$$\sigma = \frac{Zr}{a} \quad \text{and } a = \frac{\hbar^2}{4\pi^2 mc^2}$$

Charge Enclosed by Contour Surfaces

With a normalized wave function, this becomes a problem in integration of $\psi^*\psi$ over the appropriate limits:

$$f = \text{fraction enclosed} = \iiint_{\text{contour}} \psi^*\psi r^2 \sin \theta d\theta d\phi dr$$

This equation can be integrated directly when the orbital concerned has spherical symmetry with the limits: $0 < \theta < \pi$, $0 < \phi < 2\pi$ and the values of r defining the contour. In this integration each variable may be treated independently. When the contour surface has a lower symmetry, graphical integration can be used. Even this method becomes quite complex in dealing with an orbital such as the $d_{x^2 - y^2}$.

The graphical integration of the carbon $2p_z$ orbital will be described. Since there is cylindrical symmetry around the z axis the integration

$$\int_0^{2\pi} d\phi = 2\pi$$

can be included in the $\psi^*\psi$ function, hence we must evaluate the double integral:

$$f = \iint_{\text{contour}} 2\pi\psi^*\psi r^2 \sin \theta d\theta dr$$

In Figure 7 is shown the integral over r (but not θ) as

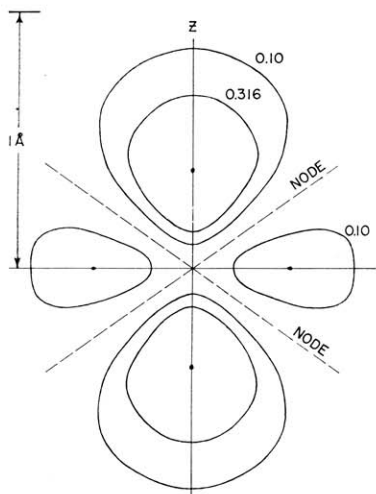


Figure 4. Contours of constant ψ^2 at 0.10 and 0.316 of maximum for a Ti(III) $3d_{z^2}$ orbital in any plane which includes the z axis. The nodes are conic surfaces making an angle $\approx 55^\circ$ with the z axis.

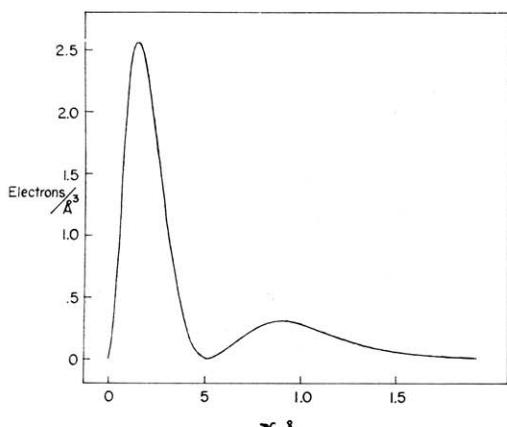


Figure 5. Electron density in a Cl $3p_z$ orbital along the z axis.

a function of the limiting value of r . This is the area under the curve $2\pi\psi^*\psi r^2$ from 0 to r . At each of the angles 0° , 20° , 40° , 60° , and 70° , the limits of r are

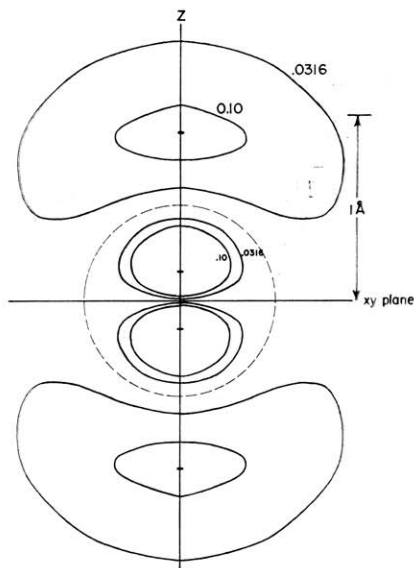


Figure 6. Contours of constant ψ^2 at 0.0316 and 0.10 of maximum for a Cl $3p_z$ orbital. The xy plane and a sphere of radius 0.52 \AA are nodal surfaces.

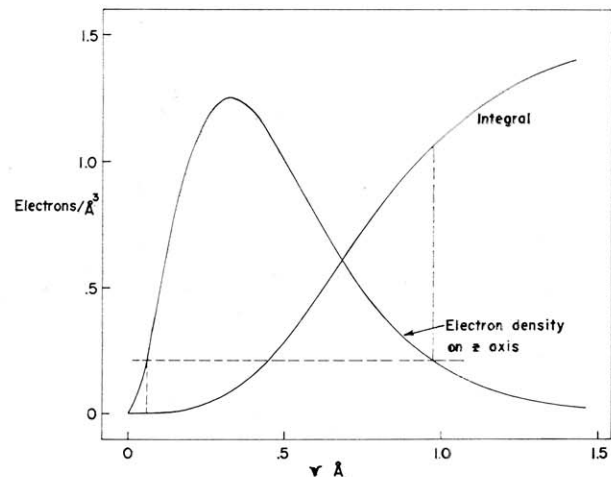


Figure 7. Electron density in a C $3p_z$ orbital along the z axis and the value of the integral $2\pi \int_0^r (\psi(r))^2 r^2 dr$ along the z axis for this orbital.

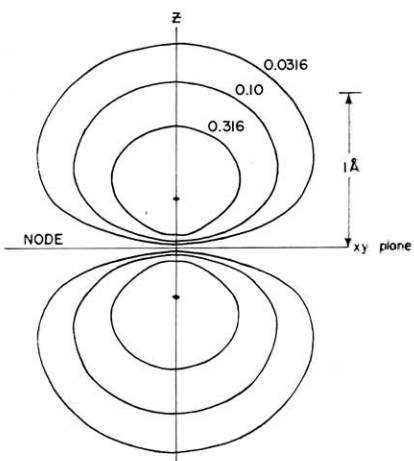


Figure 8. Contours of constant ψ^2 at 0.0316, 0.10 and 0.316 of maximum for a C $2p_z$ orbital. The xy plane is a nodal surface.

found from the electron density curve of Figure 7, and then the integral over r obtained at that angle. For example, at $\theta = 40^\circ$, with a contour at 0.10 of $\psi^* \psi_{\max}$ the limits of r are found by drawing a horizontal line at 0.10 ($\psi^* \psi_{\max} / \cos^2 40^\circ$) = 0.213 (dashed line in Fig. 7). The limits of r are thus found to be 0.065 and 0.975 Å. Transferring these limits to the area curve, we find

$$A(\theta = 40^\circ) = 2\pi \int_{r=0.065}^{0.975} \psi^* \psi r^2 dr = 1.07 - 0 = 1.07$$

Now this function is to be integrated over the angle θ :

$$f = \int_0^\pi A(\theta) \cos^2 \theta \sin \theta d\theta = - \int_0^\pi A(\theta) \cos^2 \theta d(\cos \theta)$$

This is accomplished by multiplying each value of $A(\theta)$ found from Figure 7 by $\cos^2 \theta$ and plotting the result against $\cos \theta$. In Figure 9 the resulting curves for contours at 0.316, 0.10, 0.0316, and 0.00 are shown. The last is included to provide a check on the method since with normalized wave functions, the final integration in this case must yield unity. The integration of these curves gives the fraction of the total electronic charge within a specific contour surface (the areas in Fig. 9 are to be doubled since the graph only extends from 0 to $\pi/2$ rather than to π). The results are 0.34, 0.66, 0.85, and 1.01, respectively, the last value indicating that the method is satisfactory. A smooth curve

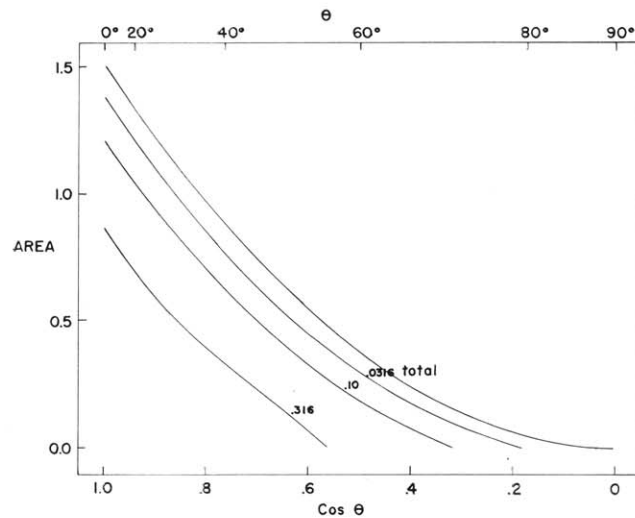


Figure 9. Values of $A(\theta) \cos^2 \theta$ versus $\cos \theta$.

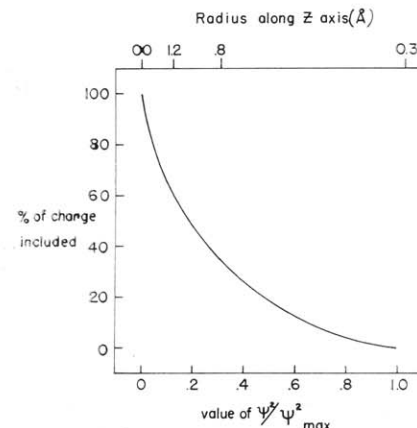


Figure 10. Percentage of electron enclosed by a constant ψ^2 contour versus the values of ψ^2/ψ_{\max} .

can be drawn through these points (Fig. 10), from which we find that to include 99% of the charge, a contour surface at $\psi^2 \psi = 0.002 \psi^2 \psi_{\max}$ would be required. This contour intersects the z axis at about $r = 2$ Å. This number provides an interesting comparison with the van der Waals radius of carbon of about 1.7 Å.

Atomic Orbital Models

Three dimensional models illustrating the contours described in the previous sections can easily be fashioned from styrofoam. Models of some orbitals of chemical interest are shown in Figure 11. Such models suffer from the disadvantage of not displaying the presence of some nodes (in the 2s and 3s orbitals for example) and also not showing the positions of highest electron density.

Figure 12 shows how it is possible to overcome these deficiencies by cutting wedges out of the models. Areas of low electron density can then be darkened.¹ The contours in Figure 12 represent the complete set of orthogonal orbitals which can be identified with the quantum numbers n , 1 and m_l for $n = 1, 2$, and 3. They are the orbitals obtained by the method of solution described by Pauling and Wilson in which the

¹ On these models black spray paint was used on the outside and a black marking pencil was used to darken the interior.

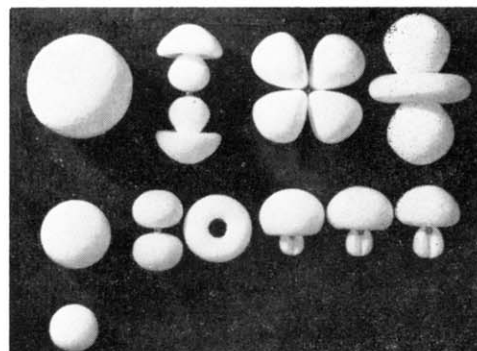


Figure 11. Models of constant ψ^2 contours of atomic orbitals of the hydrogen atom.

| | | | |
|----|---------------------------|---------------------------------|--|
| 3s | $(3p_x, 3p_y)$ | $(3d_{x^2-y^2}, 3d_{xy})$ | $(3d_{z^2} \text{ or } 3d_0)$ |
| 2s | $(2p_x, 2p_y)$ | $(2p_{+1} \text{ or } 2p_{-1})$ | $2s \quad 2sp \quad 2sp^2 \quad 2sp^3$ |
| 1s | $(2p_z \text{ or } 2p_0)$ | | |

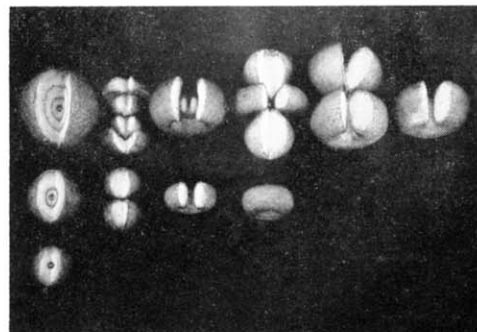


Figure 12. Atomic orbital models which have been cut away to show the presence of hidden nodes and positions of maximum electron density.

| | | | | | |
|----|--------|--------------|-----------|-----------|-----------|
| 3s | $3p_0$ | $3p_{\pm 1}$ | $3d_0$ | $3d_{+1}$ | $3d_{+2}$ |
| 2s | $2p_0$ | $2p_{+1}$ | $2p_{-1}$ | | |
| 1s | | | | | |

variable (r , θ , and ϕ) are assumed separable (5). Since other orbitals which can be obtained by taking linear combinations of these are useful for the description of polyatomic structures, they are given in Figures 13 and 14 as alternative orthogonal sets of $2p$ and $3d$ orbitals respectively. It is worth noting that values of the quantum number m_1 cannot be identified with most of these orbitals. This is still a very common textbook error.

In Figure 15 somewhat schematic models of the $1s$, $2p$, $3d$ and $4f$ orbitals are arranged to show how they are related to one another by the addition of successive planar nodes.

Molecular Orbital Models

Molecular orbitals formulated by the linear combination of atomic orbitals (LCAO) approximation are shown in Figure 16. These models are principally useful as guides in demonstrating the symmetry of the orbitals and in providing a general idea of the distribution of electron density. The bonding and antibonding orbitals which are found in first and second period homonuclear diatomic molecules are shown. The two types of π orbitals are analogous to the atomic p_0 and $p_{\pm 1}$ orbitals. In a non-linear polyatomic molecule for which the nuclei define a reference plane (e.g., ethylene), the $\pi^2 p_x$ orbital is the logical one to use, while in linear molecules, the $\pi^2 p_{\pm 1}$ orbitals with

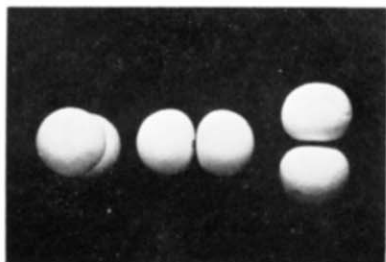


Figure 13. An alternative orthogonal set of $2p$ orbitals.

$2p_z \quad 2p_y \quad 2p_x$



Figure 14. An alternative orthogonal set of $3d$ orbitals.

| | | |
|-----------|----------------|-----------|
| $3d_{yz}$ | $3d_{x^2}$ | $3d_{xy}$ |
| $3d_{yz}$ | $3d_{x^2-y^2}$ | |

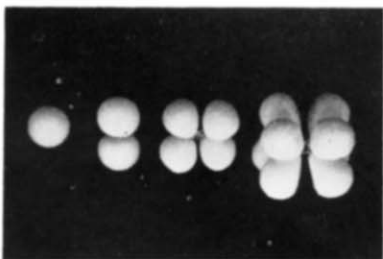


Figure 15. Somewhat schematic models of $1s$, $2p$, $3d$ and $4f$ orbitals.

cylindrical charge symmetry around the molecular axis provide a better description.

Even more schematic are the models of molecules shown in Figure 17. Unfortunately models that attempt to show contour surfaces enclosing large fractions of $\psi^* \psi$ cannot show the individual orbitals. On the other hand, contours enclosing small fractions of $\psi^* \psi$ often do not show the build-up of electron density in the region between the nuclei. No actual calculations have been attempted for these models hence, even in one model, the contour surfaces will represent different fractions of the total charge. With these

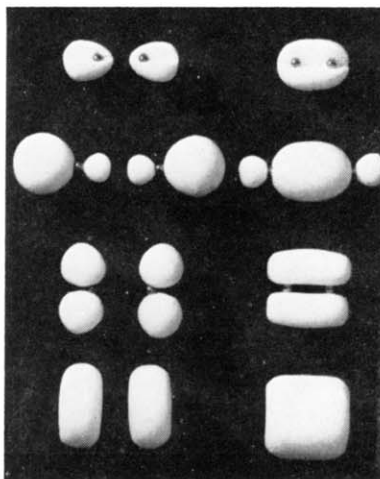


Figure 16. Models of molecular orbitals obtained by the LCAO approximation.

| Antibonding | Bonding |
|---|---|
| $\sigma^* 1s$ | $\sigma 1s$ |
| $\sigma^* 2p_z$ | $\sigma 2p_z$ |
| $(\pi^* 2p_x \text{ or } \pi^* 2p_y)$ | $(\pi 2p_x \text{ or } \pi 2p_y)$ |
| $(\pi^* 2p_{+1} \text{ or } \pi^* 2p_{-1})$ | $(\pi 2p_{+1} \text{ or } \pi 2p_{-1})$ |

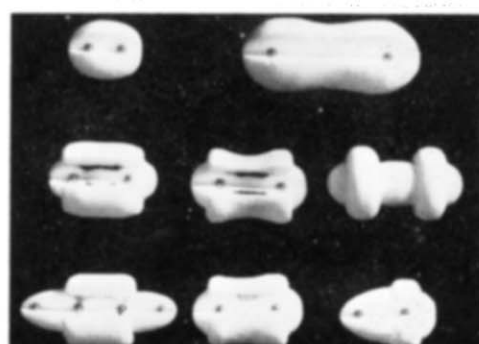


Figure 17. Somewhat schematic molecular models, cut away to show inner orbitals and nuclei.

| | |
|----------|--------|
| H_2 | Li_2 |
| N_2 | F_2 |
| C_2H_2 | NO |

limitations in mind, the models have been cut away to show the σ molecular orbitals around the molecular axis.

All of the molecules in Figure 13 have cylindrical symmetry. The description of cylindrically symmetric π orbitals is possible in most cases by using either the real p_x and p_y atomic orbitals or the complex $p_{\pm 1}$ orbitals in the LCAO description. In the NO molecule, however, one electron occupies an antibonding orbital.

For cylindrical symmetry this must be placed in one of the p_{z+1} orbitals. The change in shape of the π contours of the molecules N₂, NO, and O₂ arises from the additional contribution from the π antibonding orbitals, but the bonding and antibonding orbitals cannot, because of overlap, be shown separately (see Fig. 12).

Except for the acetylene molecule, these models have been formulated by the LCAO method without prior hybridization of the atomic orbitals. The point is controversial as indicated in recent calculations showing very little mixing of atomic orbitals even for HF, hence the concept of hybridization is used here only where required for structural reasons.

Acknowledgment

The author would like to express his thanks to Dr. Alan Bree for valuable discussions.

Literature Cited

- (1) DE BROGLIE, L., *Ann. de Phys.*, **3**, 22 (1925).
- (2) SCHRÖDINGER, E., *Ann. d. Phys.*, **79**, 360, 489 (1926); **81**, 109 (1926).
- (3) BORN, M., *Z. S. Phys.*, **38**, 803 (1926).
- (4) COHEN, I., *J. CHEM. EDUC.*, **38**, 20 (1962).
- (5) PAULING, L., AND WILSON, E., "Introduction to Quantum Mechanics," McGraw Hill, New York, **1935**.
- (6) SLATER, J. C., "Quantum Theory of Matter," McGraw-Hill, New York **1953**. Chap. 6.